Nonideality and the Nucleation of Sickle Hemoglobin

Maria Ivanova,* Ravi Jasuja,* Suzanna Kwong,† Robin W. Briehl,† and Frank A. Ferrone*
*Department of Physics, Drexel University, Philadelphia, Pennsylvania 19104, and †Department of Physiology and Biophysics and Department of Medicine, Albert Einstein College of Medicine, Bronx, New York 10461 USA

ABSTRACT The homogeneous and heterogeneous nucleation kinetics of sickle hemoglobin (HbS) have been studied for various degrees of solution crowding by substitution of cross-linked hemoglobin A, amounting to 50% of the total hemoglobin. By cross-linking hemoglobin A, hybrid formation between hemoglobin A and hemoglobin S was prevented, thus simplifying the analysis of the results. Polymerization was induced by laser photolysis, and homogeneous nucleation kinetics were determined by observation of the stochastic behavior of the onset of light scattering. Heterogeneous nucleation was determined by observing the exponential growth of the progress curves, monitored by light scattering. At concentrations between 4 and 5 mM tetramer (i.e., ~30 g/dl), the substitution of 50% HbA for HbS slows the reaction by a factor of 10^3 to 10^4. Using scaled particle theory to account for the crowding of HbA, the observed decrease in the homogeneous nucleation rate was accurately predicted, with no variation of parameters required. Heterogeneous nucleation, on the other hand, is not well described in the present formulation, and the theory for this process appears to require modification of the way in which nonideality is introduced. Nonetheless, the accuracy of the homogeneous nucleation description suggests that such an approach may be useful for other assembly processes that occur in a crowded intracellular milieu.

INTRODUCTION

Sickle hemoglobin is a natural point mutation of hemoglobin in which a charged amino acid (Glu) is replaced by a hydrophobic one (Val) on the surface of the two β subunits. This mutation leads to the assembly of long, twisted, multistranded fibers at the high concentrations typically found in red cells. The association energy is weak enough that rather high concentrations (>160 mg/ml) are required for association under conditions similar to physiological. At such concentrations, the hemoglobin molecules can no longer be considered as point objects, and significant solution nonideality must be included. Physically this reflects the fact that the center-to-center distance is significantly greater than the edge-to-edge distance of the molecules under these conditions. This nonideality has a profound effect on the physiological behavior. In vivo sickle hemoglobin aggregation occurs in the presence of oxyhemoglobin, which is incompetent to polymerization. Nonetheless, this molecule crowds the solution and so contributes to the nonideality. Likewise, the most promising therapeutic approach increases the production of fetal hemoglobin (HbF) at the expense of sickle hemoglobin (HbS) (Charache et al., 1995). While HbF does not polymerize (Sunshine et al., 1979), it, too, crowds the solution. The thermodynamic behavior of the gelation process, including the large activity coefficients required, has been thoroughly studied and appears to be well described. (Eaton and Hofrichter, 1990).

The weakness of the association energy has important consequences for the kinetics of gelation, viz., that aggregation is not favored until some minimum size aggregate is exceeded. In terms of free energy, this represents a barrier to further association. Fluctuations in aggregate size are thus required to cross this free energy barrier. The aggregate at whose size the energy maximum occurs, and for which association first becomes more likely than dissociation, is known as the nucleus. Some of the sickle cell mutation sites also occur at the fiber surface, allowing nucleation to occur on existing polymers (Mirchev and Ferrone, 1997). This latter type of nucleation is called heterogeneous, while the nucleation occurring in solution without the aid of other polymers is designated homogeneous. This nucleation-controlled reaction possesses an extraordinary sensitivity to initial conditions, depending on as much as the 50th power of initial concentration. (Ferrone et al., 1985b).

A theory has been developed for the nucleation process, and the nucleus has been modeled by considering the loss of entropy of translation and vibration of the molecules in solution, versus the energetic gains of contact energy and the vibrational entropy of motion of the monomers about their polymer sites (Ferrone et al., 1985a). Because the theory relates the nucleus to equilibrium properties and a measurable elongation rate, there is only one free parameter in this nucleation description, viz. the energy per monomer contact (Cao and Ferrone, 1997). This energy sets the magnitude of the nucleation barrier; the concentration dependence of the homogeneous nucleation process is then specified by the barrier height and other fixed parameters of the model. Agreement of the theoretical concentration dependence with what is observed has been an important validation of the soundness of the formulation.

Nonideality is included in this model without adjustable parameters. The aggregates have been approximated as

Received for publication 27 January 2000 and in final form 1 May 2000.
Address reprint requests to Dr. Frank A. Ferrone, Department of Physics and Atmospheric Science, Drexel University, 32 and Chestnut Sts., Philadelphia, PA 19104. Tel.: 215-895-2778; Fax: 215-895-5934; E-mail: fferrone@einstein.drexel.edu.

0006-3495/00/08/1016/07 $2.00

spheres, allowing the use of scaled particle theory for homogeneous nucleation, while for heterogeneous nucleation, exact cancellation of the activity coefficients for nucleus and activated complex was assumed. In the model, then, activity coefficients for the homogeneous nucleus were found to be on the order of 10^{10}. At the same time, a considerable portion of that activity coefficient is numerically canceled by the activity coefficient of the monomers. Despite the powerful effect of nonideality on the polymerization process (with two large computed terms nearly canceling), and despite the importance of nonideality to the pathophysiology of the disease, there has been no test of the accuracy of this specific description.

Probing nonideality quantitatively requires the introduction of a crowding agent whose volume and concentration are known, and which cannot copolymerize. Although dextran has been employed for such purposes (Bookchin et al., 1999), the volume of the dextran is not known a priori. Hemoglobin A is another natural crowding agent that has the same volume as HbS and will not polymerize. However, hemoglobin will naturally dissociate into $\alpha\beta$ dimers, which can reassociate into hybrids, and mixtures of liganded HbS and HbA are known to form such hybrids. Such hybrids do form polymers, and analysis of such mixtures would need to account for this effect. To avoid such complications it is possible to cross-link HbA, thereby satisfying all three criteria of known volume, absence of polymerization, and inability to undergo reproportionation. In this work we use cross-linked HbA to perturb the nucleation kinetics in ways that should be quantitatively predictable. When the results are compared with existing theories, we find that homogeneous nucleation is well described by scaled particle excluded volume theories, but that the treatment used to describe heterogeneous nucleation cannot describe the data.

MATERIALS AND METHODS

Sickle hemoglobin and hemoglobin A were prepared by column chromatography, using standard procedures. Cross-linked HbA was prepared as part of a protocol to produce cross-linked AS hybrids for other studies. Oxyhemoglobin A and S were mixed in 0.2 M bis-Tris buffer (pH 7.2), and the mixture was then converted to deoxyhemoglobin by a stream of humidified nitrogen for 1–2 h at 25°C in the presence of inositol hexaphosphate (IHP) in a 10-fold molar excess over hemoglobin. Cross-linking was performed using bis(3,5-dibromosalicyl)fumarate (DBBF) according to the procedure of Chatterjee et al. (1986) A solution of DBBF at a ratio of 1.5 molar excess over Hb was added under anaerobic conditions. The cross-linking reaction was carried out for 2 h at 37°C. At the end of the reaction, glycine was added to a final concentration of 1 M to consume any remaining reagent. The reaction mixture was then saturated with CO and passed through Sephadex G-25 to remove DBBF and IHP. The mixture was then purified by gel filtration on Sephadex G-100 (superfine) in 1 M $MgCl_2$ + 0.1% Tris (pH 7.0) to separate the uncross-linked dimers from the cross-linked tetramer fractions (Benesch and Kwong, 1991). Finally the different cross-linked fractions were separated by use of ion exchange chromatography on a High Q (Biorad) column in 25 mM Tris/bis-Tris (pH 8.0). Final purity was checked by polyacrylamide gel electrophoresis. Samples were exchanged into 0.15 M phosphate buffer (pH 7.35) on PD-10 columns and then concentrated by Centricon or Microcon concentrators.

Sample concentrations were determined by diluting the concentrated hemoglobin, using micropipettes with 1% accuracy and measuring the Soret absorption spectrum of the dilute sample in a cuvette with a 1-cm path length. Concentration determinations were repeated three or more times to further improve precision. Kinetic studies were performed on thin slides of COHb that had 50 mM sodium dithionite added to reduce any methemoglobin and scavenge oxygen.

Experiments on the kinetics of polymer formation were performed using laser photolysis of COHb, with parallel data collection (Cao and Ferrone, 1997). Photolysis is achieved by introducing the 488-nm line of a cw argon ion laser into the optical train of a horizontal microspectrophotometer. Detection is by CCD interfaced to a MacIIfx computer. The laser beam is focused on the sample by a Leitz 10× long working-distance strain-free objective and collected by an equivalent objective. Photolysis was confirmed as complete by observing the change in optical density. The photolyzed volume was determined by measuring the size of the photolysis spots and deducing the sample thickness from absorption and previously determined concentration. Polymerization was observed by detection of the scattered photolysis light. The direct beam was blocked by a spot at a point conjugate to the back aperture of the objective, and scattering proceeded around the spot. To collect data on many different regions simultaneously, the laser was passed through a mesh (Buckbee-Mears) that was subsequently imaged at the position of the field diaphragm. This created an array of photolyzed spots at the sample, of which 60–200 were observed and analyzed. To repeat the experiment the sample was moved by micrometer stage so that there was no question of the full recovery of the photolyzed region. This allowed rapid collection of large numbers of progress curves in a short time, which ensures sample stability. The temperature was regulated with a thermoelectric stage.

Homogeneous nucleation rates are obtained by analysis of the distribution of the initiation of light scattering for the different curves. To obtain such a distribution, the light scattering versus time curves were shifted in time to optimize their overlap, and the time shift was noted. Such time shifts then yield a distribution of the tenth times (time to reach 10% of maximum) of the various kinetic curves. The shifted curves could also be averaged together. This averaged curve was analyzed to yield an exponential growth rate, denoted B. For details of this procedure, the reader is referred to Mirchev (thesis). The constant B is dominated by heterogeneous nucleation, although small terms in the expression for B arise from the concentration of homogeneous nucleation as well. Specifically,

$$B^2 = J_o[g_o - df_o/dc] \quad (1)$$

in which J_o is the net rate of polymer growth, f_o is the rate of homogeneous nucleation, and g_o is the rate of heterogeneous nucleation. (Ferrone et al., 1985a).

RESULTS

Polymerization kinetics were obtained at 20°C for samples with 0%, 30%, and 50% cross-linked hemoglobin A (denoted $HbAA_{xl}$), at total hemoglobin concentrations that ranged between 4.3 and 5.2 mM (28–34 g/dl). In all cases, the same qualitative behavior was observed, viz., a distribution of tenth times, displaying exponential growth in the initial phase. For a given total Hb concentration, as the percentage of $HbAA_{xl}$ increased, the tenth times became longer and the distributions expanded. Fig. 1 shows a typical data set for c = 32 g/dl at 50% $HbAA_{xl}$. Fig. 1 *a* shows an ensemble of progress curves collected in a typical experiment. The distribution of tenth times results from the random difference in times at which nucleation occurs in the

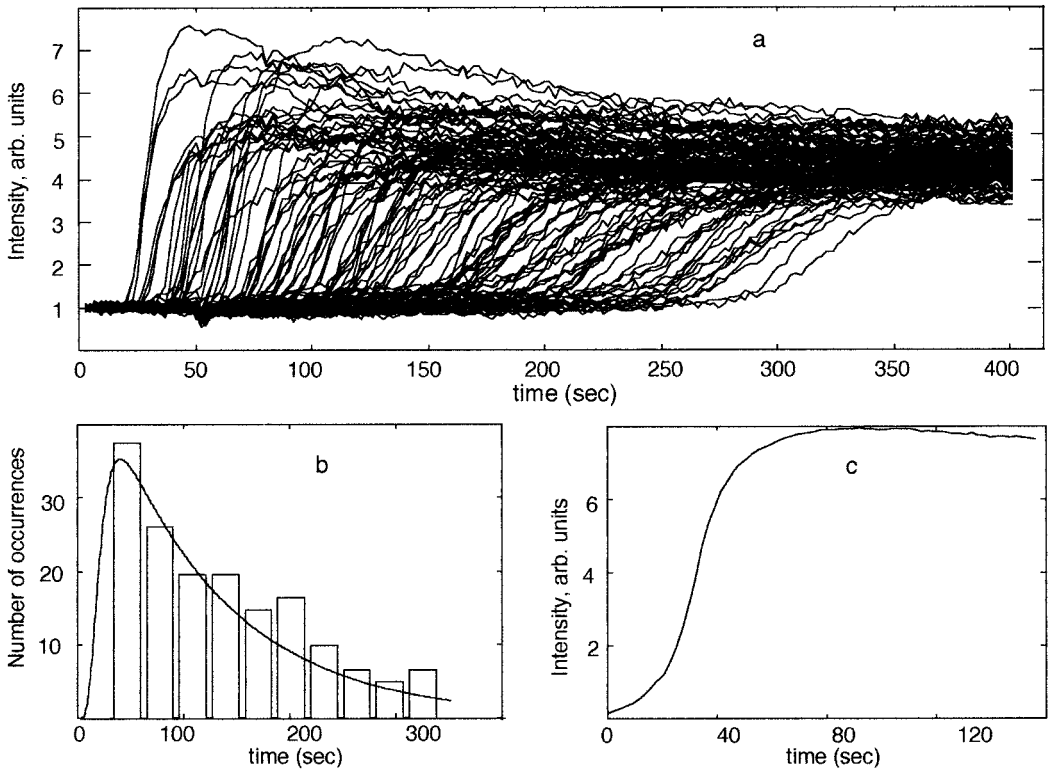

FIGURE 1 Polymerization data taken at 20°C on a sample of 32 g/dl. Photolysis creates ~200 spots in which polymerization and accompanying light scattering occurs. (*a*) Progress curves showing light scattering as a function of time after initiation. (*b*) Distribution of the tenth times of the data of *a*. The exponential tail of the distribution gives the homogeneous nucleation rate constant ζ, which here is 0.0126 s^{-1}. From this and the photolyzed volume, the homogeneous nucleation rate f_o is determined and is 1.9×10^{-8} mM/s. (*c*) Average of the progress curves in *a* after shifting by the times as shown in *b*.

various laser spots on the sample. In Fig. 1 *b* the distribution is plotted. Szabo has derived an analytic expression to relate the stochastic variation of the time of onset to the homogeneous nucleation rate (Szabo, 1988). The initial homogeneous nucleation rate is denoted by ζ and is related to the rate constant for nucleation, f_o (measured in mM/s), by multiplying f_o by the photolyzed volume V and Avogadro's number N_o, with appropriate conversion for mM, i.e.,

$$\zeta = f_o N_o V \tag{2}$$

Szabo showed that $T(t)$, the distribution of tenth times t (the time required to reach 1/10 of final value), is given by

$$T(t) = \frac{Be^{-\zeta\langle t\rangle}}{\Gamma(\zeta/B)}(1 - e^{-Bt})^n e^{-\zeta t} \tag{3}$$

in which Γ is a gamma function and n is a parameter that describes the point at which observation of the domain is made, which is equal to $e^{B\langle t\rangle}$, where $\langle t\rangle$ is the average tenth time for nonstochastic measurements. Once $t > 1/B$, the distribution decays exponentially with decay constant ζ, the rate of homogeneous nucleation. The distributions of tenth times collected here show such exponential decay, and in general this equation gives an excellent fit to all distributions collected. After the stochastic delay, the polymer concentration grows exponentially, and thus all of the progress curves should show similar behavior, once the shift in nucleation time is taken into account. Fig. 1 *c* shows the averaged progress curve once all the data of Fig. 1 *a* have been shifted to account for the differences in nucleation time and thus overlap each other. The initial points in Fig. 1 *c* show exponential growth, with rate denoted by B. This exponential parameter B is dominated by the heterogeneous nucleation rate.

Fig. 2 shows how such distributions of tenth times broaden as the fraction of $HbAA_{xl}$ is changed from 0% to 50%. All distributions have been fit by Eq. 3 to obtain the homogeneous nucleation rate, and their averaged progress curves (not shown) have also been fit to obtain B values. Average tenth times increase by ~100-fold. Even more dramatically, the exponential tail (characteristic time for homogeneous nucleation) expands by $\sim 10^4$.

Fig. 3 shows the concentration dependence of the homogeneous nucleation rate f_o for different fractions of $HbAA_{xl}$. Because of the difficulty of collecting very fast or very slow data, the data have been collected in roughly the same experimental window. Horizontal error bars are set by variation of the concentration determinations and are consistent with the rated accuracy of the pipettes used for those mea-

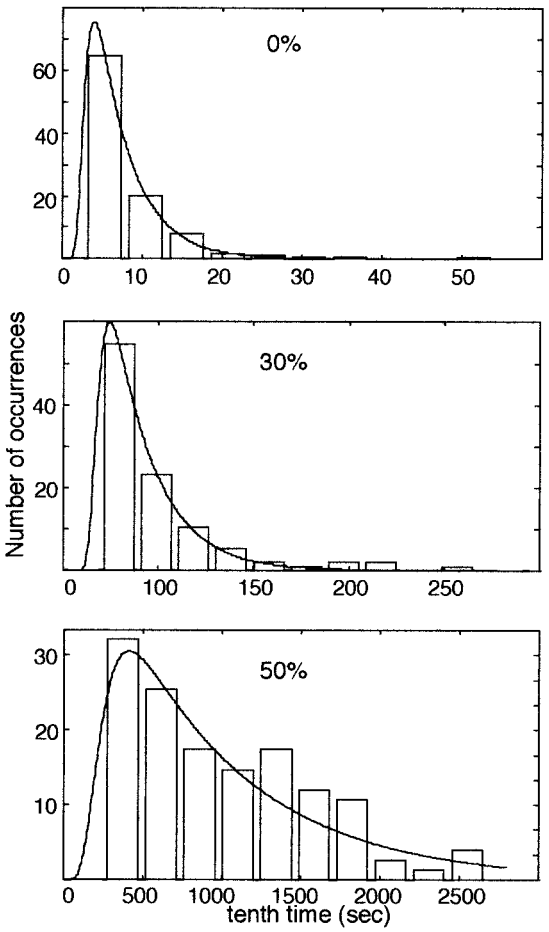

FIGURE 2 Variation in tenth time distributions as the fraction of nonpolymerizing hemoglobin increases. Each distribution is labeled with the fraction of $HbAA_{xl}$ (0%, 30%, and 50%). The broadening of the distribution is indicative of the decrease in the homogeneous nucleation rate. Total concentrations were 27.7 g/dl for 0%, 29.7 g/dl for 30%, and 31 g/dl for 50%. Note that the abscissa is not the same for all of the curves. Also note that serial collection of the 50% data (rather than by the parallel method used) would have required 200 h of collection time. Curves have been fit with Eq. 3 to determine the homogeneous nucleation rate.

surements. High concentration dependence (~50th power) is apparent for 0%, 30%, and 50% $HbAA_{xl}$. The decrease in nucleation rate is also striking as the HbS is replaced by nonpolymerizing material.

Fig. 4 shows the concentration dependence of the exponential growth rate B. Again, the same qualitative behavior is seen, viz., a strong decrease in rate as the fraction of nonpolymerizing hemoglobin increases.

Comparison with theory

To predict the effect of crowding agents it is necessary to describe the nucleation rate in fundamental terms. The homogeneous nucleation rate f_o is the result of monomer addition to a spontaneously formed nucleus. If the concentration of nuclei of size i* is denoted by c_i* with activity coefficient γ_i*, then the nucleation rate is given by

$$f_0 = k_+ \frac{\gamma_o c_o \gamma_{i^*} c_{i^*}}{\gamma^{\ddagger}} \tag{4}$$

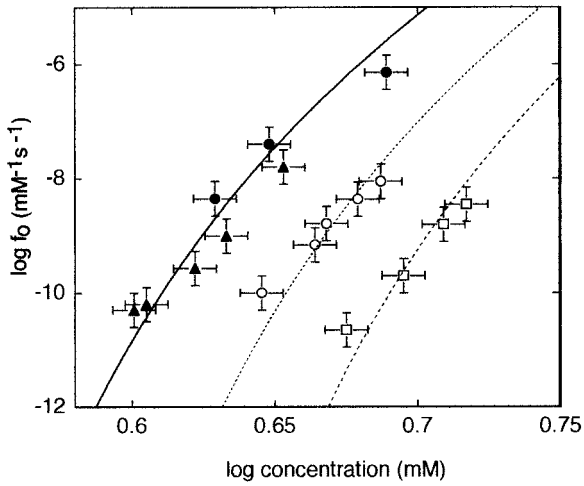

FIGURE 3 Concentration dependence of the homogeneous nucleation rate f_o for different fractions of nonpolymerizing hemoglobin. The filled symbols show the data for $X = 0$. Two different data sets are shown: data collected as the control for this project (*triangles*) and data collected and published by Cao and Ferrone (1997) (*circles*). Data collected at $X = 0.3$ are shown as open circles, and data for $X = 0.5$ are shown as open squares. The solid line through the $X = 0$ data is the fit from Cao and Ferrone. Given this fit, the model completely predicts the broken lines for $X = 0.3$ and 0.5. As can be seen, the prediction agrees very well with the data.

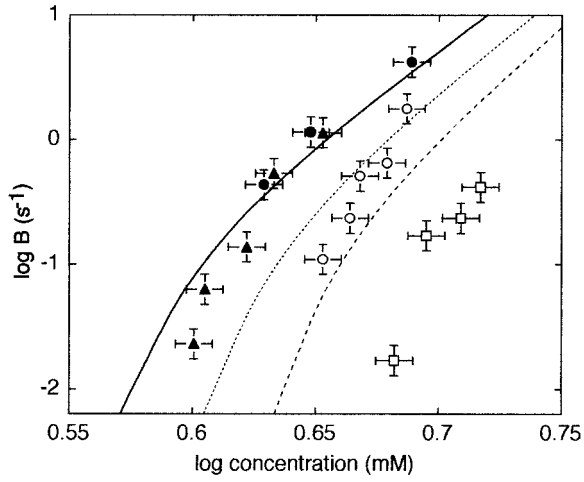

FIGURE 4 Concentration dependence of the exponential growth rate B, for different fractions of nonpolymerizing hemoglobin. Conventions are as in Fig. 3. Filled symbols show the concatenation of two data sets for $X = 0$; open circles are for $X = 0.3$, and open squares are for $X = 0.5$. The solid curve has been fit to the filled symbols, and the broken lines are the predictions for $X = 0.3$ and 0.5. The predictions in this case do not match the data. The parameter B is dominated by the heterogeneous nucleation rate as shown in Eq. 1.

in which $\gamma^{\ddagger}$ is the activity coefficient of the activated complex (cf. Eqs. 2 and A2.1 of Ferrone et al., 1985a). k_+ is the monomer addition rate. By straightforward statistical thermodynamics, c_{i^*} can be related to $\mu_{PC,}$ the chemical potential that holds the molecules within the polymer, because the nucleus is approximated as being in equilibrium with the monomers. For the sake of concise notation we introduce two variables, ξ and q. ξ contains μ_{PC} and constants specified by the geometry of the nucleation process and not varied in any fits; q contains geometrically determined constants entirely. With this notation the homogeneous nucleation rate f_o can be shown to be

$$f_o = qk_+ \frac{\gamma_o c_o \gamma_s c_s}{\gamma^{\ddagger}} \left[\frac{\ln S}{\xi}\right]^{\xi} e^{1.12\xi} \tag{5}$$

using Eqs. A2.7a and A3.13 of Ferrone et al. (1985a). Here S is the activity supersaturation at the initial concentration c_o and is defined as

$$S = \gamma c_o / \gamma_s c_s \tag{6}$$

in which c_s is the solubility and γ_s is the activity coefficient at solubility. c_o is the concentration of deoxyhemoglobin S (not total hemoglobin concentration) at the initiation of the polymerization. If X is the mole fraction of deoxyhemoglobin S, and c is the total concentration hemoglobin, then $c_o = Xc$. γ is the activity coefficient of the total hemoglobin concentration at initiation, i.e., it depends on c rather than c_o. The nucleus size, i^*, does not appear explicitly in this equation, but it is related in a very simple way to the parameters used, viz.,

$$i^* = \xi / \ln S. \tag{7}$$

The effects of crowding appear in two ways. First they appear in the activity coefficient for the monomer, γ, which only depends on the total concentration of hemoglobin. This activity coefficient is known for different concentrations from both osmotic pressure and sedimentation experiments (Ross and Minton, 1977) and has been extensively used in the study of the thermodynamics of hemoglobin S (Eaton and Hofrichter, 1990).

The second place in which nonideality is used is $\gamma^{\ddagger}$, the activity coefficient for the activated complex, an aggregate of size $i^* + 1$. Because of the dissimilar sizes of nucleus and monomer, the description for γ above cannot be used for the nucleus. Taking both nucleus and monomer as roughly spherical allows the use of scaled particle theory to determine $\gamma^{\ddagger}$ (Minton, 1981). This depends on the nucleus size (i^*) and the concentration of hemoglobin c, but once we are given such input data, $\gamma^{\ddagger}$ is fully specified with no adjustable parameters. It has been shown that

$$\begin{aligned} \ln \gamma^{\ddagger} = &-\ln(1 - Vc) + \frac{3Vc}{1 - Vc}\left(\frac{i^* + 1}{\rho}\right)^{1/3} \\ &+ \frac{3Vc + \frac{9}{2}(Vc)^2}{(1 - Vc)^2}\left(\frac{i^* + 1}{\rho}\right)^{2/3} \\ &+ \frac{Vc(1 + Vc + (Vc)^2)}{(1 - Vc)^3}\left(\frac{i^* + 1}{\rho}\right) \end{aligned} \tag{8}$$

in which V is the volume per millimole of monomer and c is the (total) monomer concentration (Ferrone et al., 1985a). The density of the nucleus relative to the monomer is given by ρ.

For a given temperature, the nucleation rate is specified by a value of k_+ and μ_{PC}. In Fig. 3, the solid line through the filled points shows the fit obtained by Cao and Ferrone (1997) (k_+ was taken from the published values of Samuel et al. (1990), so only μ_{PC} was varied). Once the nucleation rate has been determined, changes in the fraction of nonpolymerizing species will only change γ (and thus S) and $\gamma^{\ddagger}$. The theory thus makes an exact prediction of the changed homogeneous nucleation rate. The prediction is shown as the dashed lines in Fig. 3 for the $X = 0.3$ and 0.5 data, and as can be seen, the agreement is excellent. Small deviations appear at the lowest rates measured in these experiments, and further work is required to determine whether there is a systematic difference or whether the deviations represent limitations on our experimental methods.

The rate of heterogeneous nucleation is proportional to the concentration of monomers already present in polymers, and we may write it as $g_o\Delta$. Analogous to Eq. 4, we may write

$$g_o\Delta = \frac{k_+ \gamma c \gamma'_{j^*} c'_{j^*}}{\gamma'_{j^*+1}} \tag{9}$$

While this is similar in form to Eq. 4, an important new feature has appeared. Because the heterogeneous nucleus consists of an aggregate attached to a polymer, the activated complex is no longer a spherical object. The heterogeneous nucleus is also an attached aggregate and is written with a prime to distinguish it from an aggregate like the homogeneous nucleus, which is different in size.

The equilibrium for attaching an aggregate of size j^* to polymers is

$$\gamma'_{j^*} c'_{j^*} = K'_{j^*} \gamma_{j^*} c_{j^*} \gamma_p \phi \Delta \tag{10}$$

where primes indicate attached aggregates, and unprimed symbols indicate solution aggregates. K'_{j^*} is the equilibrium constant for the attachment process, Δ is the concentration of monomers in polymers, ϕ is the fraction of such polymerized monomers that can accept an aggregate, and γ_p is

the activity coefficient of the polymer with no aggregate attached.

Then Eq. 9 becomes

$$g_o\Delta = \frac{k_+\gamma c K'_{j^*}\gamma_{j^*}c_{j^*}\gamma_p\phi\Delta}{\gamma'_{j^*+1}} = k_+\gamma c K'_{j^*}\gamma_{j^*}c_{j^*}\Gamma\phi\Delta \qquad (11)$$

in which Γ is here defined as the activity coefficient for a polymer with no aggregate attached divided by the activity coefficient of a polymer with aggregate size $j^* + 1$ attached, i.e., $\Gamma = \gamma_p/\gamma'_{j^*+1}$. Γ was taken to be unity, i.e., the activity coefficients were assumed to be equal. (Ferrone et al., 1985a). Thus the only dependence of heterogeneous nucleation on nonideality is through monomer activity coefficients in the equilibrium that sets c_{j^*}.

Again, there are no parameters to be adjusted, given a fit of B to the $X = 0$ data. Fig. 4 shows the fit of log B versus log c for the $X = 0$ data and the corresponding predictions for $X = 0.3$ and 0.5. Unlike the case for homogeneous nucleation, the theory does not give a good representation of the data. For $X = 0.5$, the prediction is 10–30 times greater than the measured B value.

DISCUSSION

Homogeneous nucleation appears to be very well described by the present theoretical framework, as seen in the excellent agreement between the theory and the experimental data after we introduce crowding agents that change the rate by a factor of 10^5. This is a particularly sensitive test because the activity coefficient for the activated complex depends on nucleus size, which changes with concentration in this model. Thus not only the magnitude but the concentration dependence vary in this description. For example, over the range of concentrations from 4 to 5 mM (log c from 0.6 to 0.7), the nucleus decreases from 11 to five monomers. When 50% of the HbS is replaced by $HbAA_{xl}$, the nucleus size at 5 mM increases from five to 7.6 monomers. (A fractional nucleus size simply indicates that the nucleation reaction would first become favored at a nonintegral number of monomers.)

While it has long been recognized that solution nonideality has an important role to play in the association of sickle hemoglobin, the present data illustrate this in striking fashion. For example, at 4 mM, the activity coefficient of the activated complex increases from $\sim 10^9$ to $\sim 10^{19}$ as the fraction of nonpolymerizing hemoglobin increases to 50%. Values for $\gamma^{\ddagger}$ are very large over the whole range of X, but they are considerably offset by the monomer activity coefficient. Indeed, if one writes the nucleation rate as $k_+(\gamma^{i^*+1}/\gamma^{\ddagger})K_{i^*}c^{i^*+1}$, then the values of $\gamma^{\ddagger}$ must be compared to γ^{I^*+1}. The monomer coefficient γ itself does not depend on X because it only depends on the total hemoglobin concentration. γ^{i^*+1} changes because $i^* + 1$ increases with increasing X. The comparison of $\log_{10}\gamma^{i^*+1}$ and $\log_{10}\gamma^{\ddagger}$ is shown in Fig. 5, where it is evident that much of the activity coefficient of the activated complex is offset by the monomer coefficient. The curvature is dominated by the increase in nucleus size as X increases. Similarly, the greatest difference between γ^{i^*+1} and $\gamma^{\ddagger}$ is found at the lowest concentrations when the nucleus size is large. It is a remarkable success of the theory and, in particular, the treatment of the nonideality that such large, offsetting terms can be successfully included with no parameter adjustment.

In contrast, the effects of crowding on the heterogeneous nucleation process are not well described. This is probably because the polymer and activated complex activity coefficients do not cancel exactly, i.e., the assumption that $\Gamma = 1$ is oversimplified. More sophisticated theoretical approaches are currently under consideration, but until a successful treatment is implemented, the modeling of heterogeneous nucleation itself must also be scrutinized. Fortunately, though, the weakness in describing the heterogeneous process does not propagate into the homogeneous process, because the analysis fully decouples the two.

Consequently we believe that the description of nonideality is quite accurate over a large range. This is important

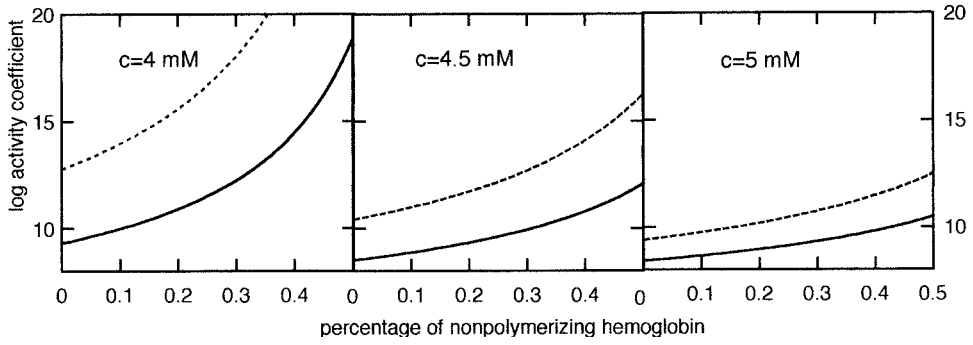

FIGURE 5 Activity coefficients as a function of the fraction of nonpolymerizing hemoglobin for three different total concentrations. The solid curve (*lower curve*) is the activity coefficient of the activated complex (nucleus plus one). The dashed curve (*upper curve*) is the activity coefficient for the monomer, raised to the power of the nucleus plus one. The increase in activity coefficient is dominated by the change in nucleus size; nuclei are larger for lower concentrations or smaller X. Note that the logs shown are base 10, although the function (Eq. 8) is natural log.

for sickle hemoglobin polymerization, as described in the Introduction, because polymerization occurs in the presence of considerable crowding, most notably of oxyhemoglobin, which does not polymerize. Crowding is not unique to the sickle hemoglobin problem. The cytoplasm is substantially volume-occupied (Fulton, 1982; Zimmerman and Trach, 1991; Cueno et al., 1992), and the varied intracellular association processes may also be influenced in this way (Kulp and Herzfeld, 1995; Madden and Herzfeld, 1993, 1994; Zimmerman and Minton, 1993). Most intriguing is the recent suggestion by Minton that amyloid formation might also be affected by the crowding of the intracellular milieu. (Minton, 2000). The experimental tests presented here strengthen the utility of excluded volume theories as an accurate description of the kinetics of association in crowded media.

REFERENCES

Benesch, R., and S. Kwong. 1991. Hemoglobin tetramers stabilized by a single intramolecular cross-link. *J. Protein Chem.* 10:503–510.

Bookchin, R., T. Balazs, Z. Wang, R. Josephs, and V. Lew. 1999. Polymer structure and solubility of deoxyhemoglobin S in the presence of high concentrations of volume-excluding 70-kDa dextran. *J. Biol. Chem.* 274:6689–6697.

Cao, Z., and F. A. Ferrone. 1997. Homogeneous nucleation in sickle hemoglobin. Stochastic measurements with a parallel method. *Biophys. J.* 72:343–372.

Charache, S., M. L. Perrin, R. D. Morre, G. J. Dover, F. B. Barton, S. V. Eckert, R. P. McMahon, and D. R. Bonds. 1995. Effect of hydroxyurea on the frequency of painful crises in sickle cell anemia. *N. Engl. J. Med.* 332:1317–1322.

Chatterjee, R., E. V. Welty, R. Y. Walder, S. L. Pruitt, P. H. Rogers, A. Arnone, and J. A. Walder. 1986. Isolation and characterization of a new hemoglobin derivative cross-linked between the α chains (lysine 99α1-lysine 99α2). *J. Biol. Chem.* 261:9929–9937.

Cueno, P., E. Magri, A. Verzola, and E. Grazi. 1992. Macromolecular crowding is a primary factor in the organization of the cytoskeleton. *Biochem. J.* 281:507–512.

Eaton, W. A., and J. Hofrichter. 1990. Sickle cell hemoglobin polymerization. *Adv. Protein Chem.* 40:63–280.

Ferrone, F. A., J. Hofrichter, and W. A. Eaton. 1985a. Kinetics of sickle hemoglobin polymerization. II. A double nucleation mechanism. *J. Mol. Biol.* 183:611–631.

Ferrone, F. A., J. Hofrichter, and W. A. Eaton. 1985b. Kinetics of sickle hemoglobin polymerization. I. Studies using temperature-jump and laser photolysis techniques. *J. Mol. Biol.* 183:591–610.

Fulton, A. B. 1982. How crowded is the cytoplasm? *Cell.* 30:345–347.

Kulp, D. T., and J. Herzfeld. 1995. Crowding-induced organization of cytoskeletal elements. III. Spontaneous bundling and sorting of self-assembled filaments with different flexibilities. *Biophys. Chem.* 57: 93–102.

Madden, T. L., and J. Herzfeld. 1993. Crowding-induced organization of cytoskeletal elements. I. Spontaneous demixing of cytosolic proteins and model filaments to form filament bundles. *Biophys. J.* 65:1147–1154.

Madden, T. L., and J. Herzfeld. 1994. Crowding-induced organization of cytoskeletal elements. II. Dissolution of spontaneously formed filament bundles by capping proteins. *J. Cell Biol.* 126:169–174.

Minton, A. P. 1981. Excluded volume as a determinant of macromolecular structure and reactivity. *Biopolymers.* 20:2093–2120.

Minton, A. P. 2000. Implications of macromolecular crowding for protein assembly. *Curr. Opin. Struct. Biol.* (in press).

Mirchev, R. 1999. Heterogeneous nucleation of sickle hemoglobin. Ph.D. thesis, Drexel University, Philadelphia, PA.

Mirchev, R., and F. A. Ferrone. 1997. The structural origin of heterogeneous nucleation and polymer cross linking in sickle hemoglobin. *J. Mol. Biol.* 265:475–479.

Ross, P. D., and A. P. Minton. 1977. Analysis of non-ideal behavior in concentrated hemoglobin solutions. *J. Mol. Biol.* 112:437–452.

Samuel, R. E., E. D. Salmon, and R. W. Briehl. 1990. Nucleation and growth of fibres and gel formation in sickle cell haemoglobin. *Nature.* 345:833–835.

Sunshine, H. R., J. Hofrichter, and W. A. Eaton. 1979. Gelation of sickle cell hemoglobin in mixtures with normal adult and fetal hemoglobins. *J. Mol. Biol.* 133:435–467.

Szabo, A. 1988. Fluctuations in the polymerization of sickle hemoglobin: a simple analytical model. *J. Mol. Biol.* 199:539–542.

Zimmerman, S. B., and A. P. Minton. 1993. Macromolecular crowding: biochemical and physiological consequences. *Annu. Rev. Biophys. Biomol. Struct.* 22:27–65.

Zimmerman, S. B., and S. O. Trach. 1991. Estimation of macromolecule concentrations and excluded volume effects for the cytoplasm of *E. coli. J. Mol. Biol.* 222:599–620.